NASA/TP—2007–215079

Prediction of Geomagnetic Activity and Key Parameters in High-Latitude Ionosphere—Basic Elements

W. Lyatsky
Oak Ridge Associated Universities, Oak Ridge, Tennessee

G.V. Khazanov
Marshall Space Flight Center, Marshall Space Flight Center, Alabama

October 2007

The NASA STI Program…in Profile

Since its founding, NASA has been dedicated to the advancement of aeronautics and space science. The NASA Scientific and Technical Information (STI) Program Office plays a key part in helping NASA maintain this important role.

The NASA STI program operates under the auspices of the Agency Chief Information Officer. It collects, organizes, provides for archiving, and disseminates NASA's STI. The NASA STI program provides access to the NASA Aeronautics and Space Database and its public interface, the NASA Technical Report Server, thus providing one of the largest collections of aeronautical and space science STI in the world. Results are published in both non-NASA channels and by NASA in the NASA STI Report Series, which includes the following report types:

- TECHNICAL PUBLICATION. Reports of completed research or a major significant phase of research that present the results of NASA programs and include extensive data or theoretical analysis. Includes compilations of significant scientific and technical data and information deemed to be of continuing reference value. NASA's counterpart of peer-reviewed formal professional papers but has less stringent limitations on manuscript length and extent of graphic presentations.

- TECHNICAL MEMORANDUM. Scientific and technical findings that are preliminary or of specialized interest, e.g., quick release reports, working papers, and bibliographies that contain minimal annotation. Does not contain extensive analysis.

- CONTRACTOR REPORT. Scientific and technical findings by NASA-sponsored contractors and grantees.

- CONFERENCE PUBLICATION. Collected papers from scientific and technical conferences, symposia, seminars, or other meetings sponsored or cosponsored by NASA.

- SPECIAL PUBLICATION. Scientific, technical, or historical information from NASA programs, projects, and missions, often concerned with subjects having substantial public interest.

- TECHNICAL TRANSLATION. English-language translations of foreign scientific and technical material pertinent to NASA's mission.

Specialized services also include creating custom thesauri, building customized databases, and organizing and publishing research results.

For more information about the NASA STI program, see the following:

- Access the NASA STI program home page at <http://www.sti.nasa.gov>

- E-mail your question via the Internet to <help@sti.nasa.gov>

- Fax your question to the NASA STI Help Desk at 301–621–0134

- Phone the NASA STI Help Desk at 301–621–0390

- Write to:
  NASA STI Help Desk
  NASA Center for AeroSpace Information
  7115 Standard Drive
  Hanover, MD 21076–1320

NASA/TP—2007–215079

Prediction of Geomagnetic Activity and Key Parameters in High-Latitude Ionosphere—Basic Elements

W. Lyatsky
Oak Ridge Associated Universities, Oak Ridge, Tennessee

G.V. Khazanov
Marshall Space Flight Center, Marshall Space Flight Center, Alabama

National Aeronautics and
Space Administration

Marshall Space Flight Center • MSFC, Alabama 35812

October 2007

Acknowledgments

We are grateful to Aaron Ridley for kindly providing us with data on cross-polar cap potential and total hemispheric Joule heating in the Northern Hemisphere computed with the assimilative mapping of ionospheric electrodynamics technique, and Arjun Tan for fruitful collaboration. We also gratefully acknowledge invaluable efforts of the Goddard Space Flight Center staff, the National Geophysical Data Center, the Danish Meteorological Institute, and the World Data Center, Kyoto, Japan, in providing solar wind data, geomagnetic activity indices, and data from geomagnetic observatories. This study was partially funded from NASA grant NAG5–11995.

Available from:

NASA Center for AeroSpace Information
7115 Standard Drive
Hanover, MD 21076–1320
301–621–0390

This report is also available in electronic form at
<https://www2.sti.nasa.gov>

TABLE OF CONTENTS

LIST OF FIGURES

LIST OF FIGURES (Continued)

LIST OF ACRONYMS

AE	auroral electrojet index of geomagnetic activity
AL	auroral electrojet index of geomagnetic activity
AMIE	assimilative mapping of ionospheric electrodynamics
CPC	cross-polar-cap (potential drop)
Dst	low latitude index of geomagnetic activity
F function	a solar wind-geomagnetic activity coupling function
*F** function	a solar wind-geomagnetic activity dimensionless coupling function
IMF	interplanetary magnetic field
JH	Joule heating
Kp	subauroral index (of geomagnetic activity)
OMNI	a multisource, hourly resolution compilation of near-Earth energetic particle and solar wind magnetic field and plasma data
PC	polar cap index of geomagnetic activity
PM	polar magnetic index of geomagnetic activity
SuperDARN	Super Dual Auroral Radar Network
TP	Technical Publication
UT	universal time

NOMENCLATURE

A	quantity
a	coefficient
A_0	measured magnetic field
$\mathbf{B}$	magnetic field vector
b	coefficient
B_z	IMF component along the z-axis in solar-magnetospheric frame
B_y	IMF component along the y-axis in solar-magnetospheric frame IMF
B_{yz}	IMF component in the y-z plane in solar-magnetospheric frame IMF
C	constant
c	coefficient
D	day of year
E	electric field
$\mathbf{e}_b$	a unit vector corresponding to the best correlation
F	solar wind-geomagnetic activity coupling function
F^*	dimensionless solar wind-geomagnetic activity coupling function
F_{visc}	coupling function accounting for a contribution from viscous interaction
f	a function
g	corrective function of season and UT
$\mathbf{H}$	geomagnetic field vector measured on the ground
H_b	geomagnetic field component of magnetic disturbances across the transpolar equivalent ionospheric current
$H_\perp$	geomagnetic field in the horizontal plane
H_z	geomagnetic field component along the vertical (downward) direction
l	a number—upper level of summing
M	a quantity
m	arbitrary value
n	solar wind plasma density number; arbitrary value
R	correlation coefficient

NOMENCLATURE (Continued)

R^2	goodness of fit
r	a number—upper level of summing
t	time
U	electric potential drop
V_{sw}	solar wind velocity
ν	power
X	geomagnetic field component along the x-axis
x	horizontal (northward) axis
Y	geomagnetic field component along the y-axis
y	azimuthal axis
Z	geomagnetic field component along the z-axis
z	vertical axis
α	arbitrary value
Δ	increment
γ	an exponent
φ	clock angle in the horizontal x-y plane on the ground
Λ	geomagnetic latitude
θ	clock angle in solar-magnetosphere frame in the y-z plane between the z (northward) axis and the $\mathbf{B}_{yz}$ vector

TECHNICAL PUBLICATION

PREDICTION OF GEOMAGNETIC ACTIVITY AND KEY PARAMETERS IN HIGH-LATITUDE IONOSPHERE—BASIC ELEMENTS

1. INTRODUCTION

Prediction of geomagnetic activity and related events in the Earth's magnetosphere and ionosphere is an important task of the Space Weather program. Relatively long-term (for several days and longer) prediction of geomagnetic activity is usually based on observations of the Sun while short-term (about 1–2 hr) prediction is based on upstream solar wind and interplanetary magnetic field (IMF) data, measured with spacecraft at the distance of about 100 to 200 Earth radii sunward. The last, more reliable prediction method will primarily be used here.

In general form, the prediction formula can be expressed as:[1]

$$M(t) = \sum_{m=1}^{r} a_m M(t - m\Delta t) + \sum_{m=0}^{l} b_m F(t - m\Delta t) \ , \tag{1}$$

where M is a predicted value at the time (t), $M(t-m\Delta t)$ is this value at a previous time ($t-m\Delta t$), F is a function that affects the M value and taken at ($t-m\Delta t$), and a_m and b_m are some coefficients. In the linear approach, the coefficients a_m and b_m are assumed to be constant, while in a nonlinear approach, these coefficients may be dependent on values of M and F. The prediction includes the determination of the F function, the coefficients a_m and b_m, and the integration time. In the prediction of geomagnetic activity from solar wind data, different coupling functions (F) are used, which are the combinations of solar wind parameters affecting the magnetosphere.[1–6] The second term in equation (1) is related to a source. The first term is accounting for the value under investigation taken for a previous time interval.

The prediction also includes predicting (evaluating) some quantities that cannot easily be obtained but may be predicted from available experimental data using results of correlation analysis. For instance, the cross-polar cap (CPC) electric potential is a key parameter that shows an electric energy flux entering the dayside ionosphere from the solar wind. The CPC voltage cannot be reliably monitored. Computing the CPC voltage is an inverse problem that includes a complicated technique using geomagnetic field data from many geomagnetic observatories.[7,8] As a result, monitoring the CPC voltage at present is not possible; however, CPC voltage may be predicted with high reliability from upstream solar wind/IMF data and appropriate geomagnetic activity indices.

Prediction reliability is dependent on both prediction method and the elements included. The two main elements are an appropriate geomagnetic activity index and coupling function—the combination of

solar wind parameters providing the best-fit correlation between upstream solar wind/IMF data and geomagnetic activity. The appropriate choice of these two elements is imperative for any reliable prediction model. The first element, a geomagnetic activity index, should be available in near-real time and have a clear meaning as well as good, reliable correlation with upstream solar wind/IMF data. The second element is the coupling function, a combination of solar wind/IMF parameters providing the best correlation between upstream solar wind/IMF data and geomagnetic activity indices.

The purpose of this Technical Paper (TP) is to reanalyze and improve these two key elements—the appropriate geomagnetic activity index and the solar wind coupling function—which is an important step in improving the prediction reliability of geomagnetic activity and related events in the Earth's magnetosphere, ionosphere, and thermosphere.

A new geomagnetic activity index has been developed that shows much better correlation with upstream solar wind/IMF data than other existing indices. A new version of the solar wind coupling function, which accounts for both solar wind electric field, penetrating into the magnetosphere, and the effect of solar wind density and pressure, has been developed. This coupling function shows high, stable correlation with geomagnetic activity and related events in the magnetosphere and ionosphere. Correlation of the new index with the solar wind coupling function, other indices, such as the auroral electrojet (AL) and the subauroral (Kp) indices, and related disturbances in the Earth's ionosphere have been discussed. Reliable prediction capabilities of some key parameters in the Earth's magnetosphere and ionosphere, such as the CPC voltage and total hemispheric Joule heating (JH) in the high-latitude ionosphere, has been shown. These quantities are used as important input parameters for modeling the magnetospheric, ionospheric, and thermospheric processes, and their prediction reliability is very important.

2. POLAR MAGNETIC INDEX OF GEOMAGNETIC ACTIVITY

2.1 Introduction

Geomagnetic activity indices, used for measuring the level of geomagnetic activity, are calculated from measurements of geomagnetic disturbances at specific geomagnetic observatories. Various indices show different types of geomagnetic activity.[9–12] The auroral electrojet (AL and AE) indices show geomagnetic activity in the auroral zone related to substorm activity. The subauroral (Kp) index shows geomagnetic activity at middle latitudes. The low-latitude (Dst) index shows the intensity of the ring current produced by energetic particles in the magnetosphere. The polar cap (PC) index measures geomagnetic activity produced by overhead ionospheric currents and field-aligned currents in the north and south polar caps. Since the primary source of geomagnetic disturbances is the solar wind, geomagnetic activity indices show the clear correlation with upstream solar wind/IMF data.

The existing geomagnetic activity indices were developed many years ago, when knowledge of the magnetosphere and ionosphere was insufficient, and improving the reliability of space weather prediction requires the development of more appropriate indices. Main requirements for improving such indices are as follows:

- Should have a better, more stable correlation with upstream solar wind/IMF data.

- Should have good correlation with key ionospheric and magnetospheric parameters, such as CPC potential drop, Joule heating, and others, which are used as input parameters for modeling the processes in the magnetosphere, ionosphere, and thermosphere.

- Should be available in near real time.

In this TP, study results of a new, polar magnetic (PM) index of geomagnetic activity is shown. This index was computed from magnetic field measurements from two near-pole geomagnetic observatories—Thule, Greenland, and Vostok, Antarctica—the same observatories that are used for deriving the existing PC index, but a different method for deriving the PM index was used. As a result, the PM index shows a much better correlation with the solar wind coupling function and related events than do other existing indices, including the PC index. Although the PM index was computed from both observatories in two hemispheres, the data from the Vostok Observatory are only partially available for the interval considered (1995–2004), and in this TP, only results obtained from the Thule Observatory—related to the Northern Hemisphere—will be considered.

The most important distinction of the PM index from the existing PC index consists of accounting for the contribution from the transpolar (CPC) equivalent ionospheric current to geomagnetic activity and related events, even when the transpolar current deviates significantly from its average direction. This leads to a significant increase in the correlation between the PM index and both upstream solar wind

data and key ground-measured parameters, such as CPC potential and Joule heating in the high-latitude ionosphere, which are used as input parameters for modeling the magnetospheric, ionospheric, and thermospheric processes.

2.2 Polar Magnetic Index Calculation Method

The existing PC index was introduced for measuring the transpolar equivalent ionospheric current, which is an important feature of high-latitude geomagnetic disturbances. This index is calculated from measurements at two near-pole geomagnetic stations—Thule in the Northern Hemisphere (corrected geomagnetic latitude $\Lambda \approx 86.5°$) and Vostok in the Southern Hemisphere ($\Lambda \approx -83.4°$). The PC index derived from magnetic field measurements in the north polar cap is related mostly to geomagnetic activity in the Northern Hemisphere, while the index derived from magnetic field measurements in the south polar cap is related mostly to the Southern Hemisphere.

The transpolar current commonly points between noon and dawn, so that the vector of magnetic disturbances on the ground points somewhere between noon and dusk. For deriving the PC index, the component of magnetic disturbances (H_b) across a statistically-average direction of the transpolar electric current is computed:[11]

$$H_b = \mathbf{H} \bullet \mathbf{e}_b \ , \tag{2}$$

where $\mathbf{H}$ is the vector of a geomagnetic disturbance in the horizontal plane and $\mathbf{e}_b$ is the unit vector related to the transpolar current in a specific universal time (UT) and season, and directed across this transpolar current. The 'true' directions of the transpolar current and the $\mathbf{e}_b$ vector are found when the H_b values show the best correlation with upstream solar wind/IMF data.

Thus, the PC index shows the component of geomagnetic perturbations across an average direction of the transpolar current. This method gives relatively good results when the direction of the transpolar current is close to its average direction. In other cases, it leads to a significant error. Therefore, for evaluating the magnitude of the transpolar current, another method is used, which provides good results even when the direction of the transpolar current differs significantly from its average direction.

Equation (2), used for computing the PC index, suggests that the transpolar current, flowing across a statistically-average direction of this current, produces no geomagnetic activity. This approach underestimates the level of geomagnetic activity predicted from the PC index, since the transpolar equivalent ionospheric current contributes to geomagnetic activity even when it is significantly deflected from its average direction. To reduce this incorrectness, a new PM index was computed.

Instead of using equation (2) for the calculation of the PM index, the Akasofu function [2,5,13] was used, which derives the effectiveness of reconnection at dayside magnetopause when the IMF vector may be significantly deflected from the z-axis, making the problem close to the case under consideration. The following quantity was computed for deriving the PM index:

$$\Delta H = H_{\perp} \sin^{\nu}(\varphi/2) \ , \tag{3}$$

where $H_\perp$ is a total geomagnetic disturbance in the horizontal plane; φ is the angle measured from the direction, opposite the transpolar current, to its actual direction; and ν is the power derived from experimental data to provide the best correlation between ΔH and upstream solar wind/IMF data, which gives $\nu \approx 3$. The angle (φ) is derived from experimental data for each UT hour and season. If the transpolar current is along its averaged direction, $\varphi = \pi$. In this case, equation (3) coincides with equation (2).

The ΔH quantities derived from equation (3) may be significantly different from H_b quantities that are used for calculating the PC index. For instance, if the transpolar current is deflected from its average direction by the angle of $\pi/2$, $H_b = 0$ is obtained from equation (2), while from equation (3), $\Delta H \approx 0.35\, H_\perp$ is obtained, so that the contribution from the transpolar current to ΔH remains very significant.

The ΔH quantity may also be written as

$$\Delta H = H_\perp \sin^3(\varphi/2) = H_\perp \sin^3 \left[0.5 \operatorname{acos}\left(-H_b/H_\perp\right)\right] . \tag{4}$$

The values of ΔH may be used for a rough estimate of the PM index. The correlation with upstream solar wind/IMF data, however, is better while accounting for the magnetic field vertical H_z component. Then, the finale formula for the PM index becomes the following:

$$\mathrm{PM} = \left\{ H_\perp \sin^3 \left[0.5 \operatorname{acos}\left(-\mathrm{H_b}/\mathrm{H_\perp}\right)\right] + 0.25 \left| H_z \right| \right\} f(\mathrm{UT}, \mathrm{season}) , \tag{5}$$

where the factor 0.25 has been chosen to provide the best correlation of the resulting PM index with upstream solar wind/IMF data, and f(UT, season) is a function, reducing the effect of UT and season, which are very strong at high latitudes,[14,15] on ionospheric conductance and currents.

Geomagnetic disturbances related to the sign (but not the absolute value) of the interplanetary magnetic field (IMF B_y) related to the so-called Svalgaard-Mansurov effect,[16,17] were reduced. This effect is associated with a single-current vortex located in the polar cap and changing its direction with the sign of IMF B_y. This current does not contribute to the total transpolar current but produces a significant spread in the correlation between computed ΔH fields and upstream solar wind data.

For calculation of the PM index, the x, y, z coordinate system was used, where in the Northern Hemisphere, the axis x is northward, axis y is eastward, and axis z is downward. The secular and quiet-day diurnal variations of the magnetic field were removed, and the UT/season variations reduced. To reduce the UT/season variations, a simple analytical formula was used:

$$A = A_0 f(\mathrm{UT}, \mathrm{season}) , \tag{6}$$

where A_0 is an actual measured magnetic field, A is a corrected magnetic field, and f(UT, season) is as follows:

$$f(\mathrm{UT}, \mathrm{season}) = 1 - 0.3 \cos\left[2\pi\,(D - 174)/365\right] - 0.5 \cos\left[2\pi\,(\mathrm{UT} - 15.5)/24\right] , \tag{7}$$

where D is the day of year and UT is measured in hours.

To account for the UT/seasonal variation of the average direction of the transpolar current and H_b field, when computing the H_b field, the following expression was used:

$$H_b = X\cos\left[2\pi\left(\mathrm{UT}-g\right)/24\right]+Y\sin\left[2\pi\left(\mathrm{UT}-g\right)/24\right] \ , \tag{8}$$

where X and Y are the corrected magnetic field disturbances along the x (northward) and y (eastward) axes, UT is universal time in hours, and g is a corrective function of season and UT that was derived from experimental data. The g function was found from the following expression:

$$g = 7.2 + 0.5\cos\left[2\pi\left(D-174\right)/365\right] - 0.12\ \cos\left[2\pi\left(\mathrm{UT}-11.5\right)/24\right] \ . \tag{9}$$

The coefficients in equation (9) were derived to provide the best correlation between the PM index and upstream solar wind/IMF data.

As mentioned above, for deriving the PC index, only the H_b magnetic fields were used, which underestimates a real CPC convection flow and a real transpolar current due to significant deflections of the convection flow and the transpolar current from their average directions. The method used for deriving the PM index is accounting for possible deflections of the transpolar current and related magnetic field in the polar cap from their average directions. This method provides a more accurate evaluation of the transpolar current responsible for geomagnetic activity not only in the polar cap but also at lower latitudes.

Figures 1 and 2 show two examples of the correlation of the H_b field and PC/PM indices with upstream solar wind/IMF data. These figures demonstrate a significant increase in the correlation between the PM index and the coupling function (F^*) as compared with the correlation of the H_b magnetic field and the PC index with the same F^* function. The dimensionless coupling function (F^*) provides the best correlation between geomagnetic activity indices and upstream solar wind/IMF data. The explanation for this coupling function is presented in section 3.

Figure 1 shows the correlation of (a) the magnetic field (H_b) with the coupling function (F^*) and (b) the PC index with the coupling function (F^*) for 2001. The correlation patterns for H_b and the PC index versus F^* are similar, and correlation coefficients differ insignificantly. Panel (c) shows the correlation between the PM index and the coupling function (F^*). One can see that the correlation of the PM index with the coupling function (F^*) is significantly higher. Goodness of fit (R^2) increases to ~0.71, which corresponds to the correlation coefficient $R \approx 0.84$.

Figure 2 shows the correlation patterns for (a) H_b versus F^* and (b) the PC index versus F^* for 2002. Panel (c) shows the correlation between the PM index and the F^* function. Again, the correlation of the PM index versus the F^* function increases significantly. R^2 also increases to ~0.7.

The correlation between the PM index and coupling function (F^*) is better than that between H_b/PC and the F^* function for each year from 1995 through 2004, and the goodness of fit (R^2) varies from ~0.8 (near solar minimum) to ~0.7 (near solar maximum), which corresponds to the variation of the correlation coefficient (R) from ~0.9 to ~0.84.

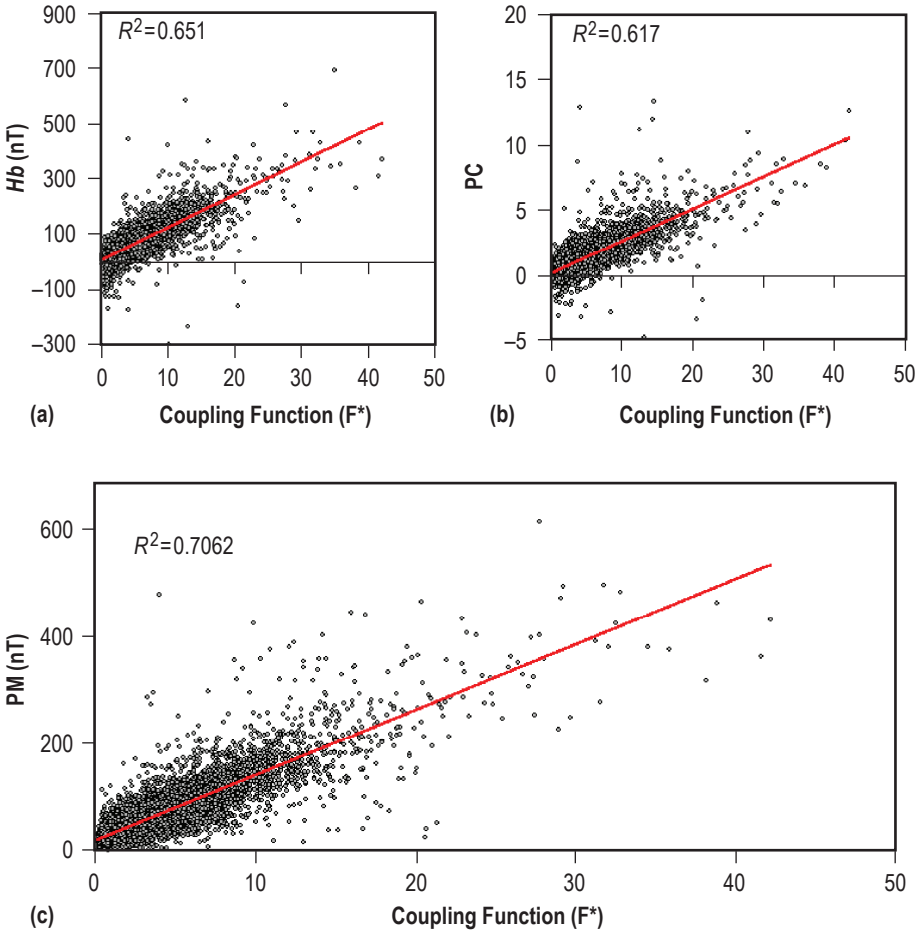

Figure 1. Correlation of the coupling function (F^*) with hourly mean values of (a) magnetic fields (H_b), (b) the PC index, and (c) the PM index for 2001.

In addition to the high correlation with upstream solar wind/IMF data, the PM index also shows high correlation with key parameters in the magnetosphere and ionosphere, such as the Kp and Dst indices, CPC potential drop, and Joule heating released in the high-latitude ionosphere. These effects will be covered in the next sections.

For computing the PM index, 1-hr, and for some cases, 15-min, measurements from high-latitude Thule (corrected geomagnetic latitude $\Lambda \approx 85°$) and Vostok ($\Lambda \approx -83°$) observatories in the Northern and Southern Hemispheres were used, respectively, for 10 yr (1995–2004). Although the PM index in both polar caps was computed, the results obtained for the Northern Hemisphere only are considered here. (The magnetic field measurements from the Southern Hemisphere are not available for all years.) The magnetic field data and geomagnetic activity indices were obtained from the World Data Centers in Kyoto, Japan, and the Danish Meteorological Institute, Denmark, at Web sites <http://swdcwww.kugi.kyoto-u.ac.jp> and <http://web.dmi.dk>, respectively. Also used were the OMNI solar wind/IMF data, available from Goddard Space Flight Center at <ftp://nssdcftp.gsfc.nasa.gov/spacecraft_data/omni/>. In this TP, the hourly mean values of the geomagnetic field and upstream solar wind/IMF data were used for analysis.

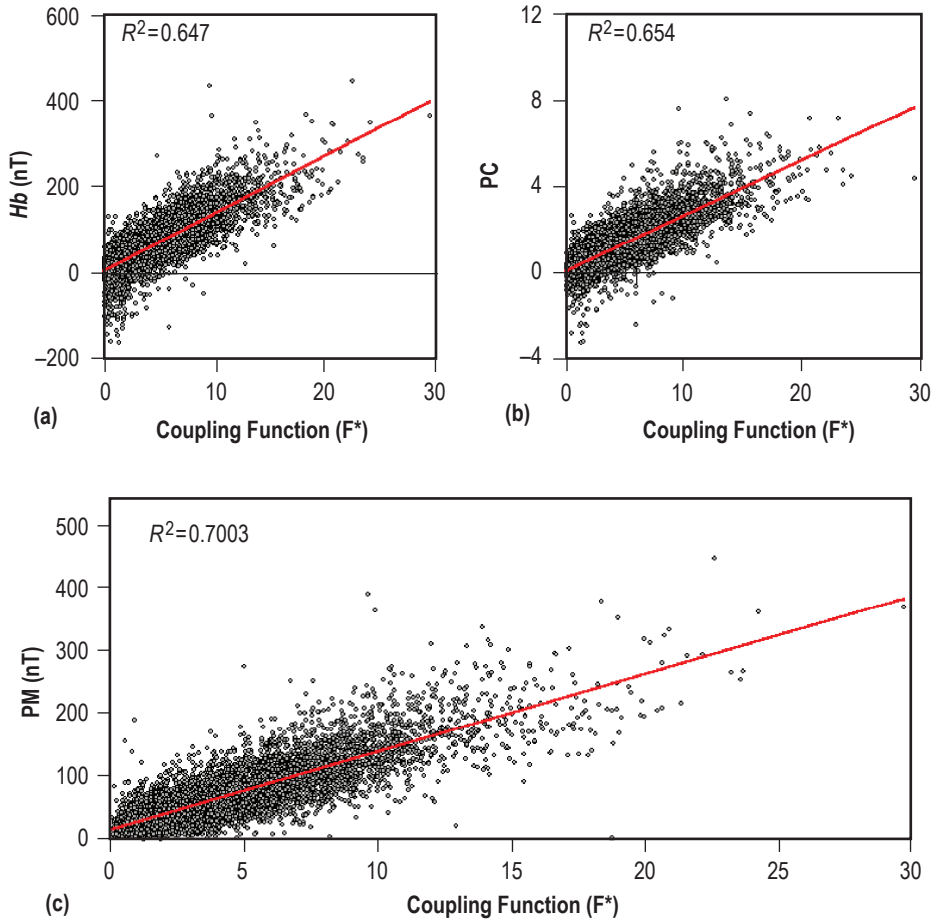

Figure 2. Correlation of the coupling function (F^*) with hourly mean values of (a) magnetic fields (H_b), (b) the PC index, and (c) the PM index for 2002.

3. COUPLING FUNCTION

3.1 Existing and New Coupling Functions

To improve the prediction of geomagnetic activity, it is also necessary to derive an appropriate solar wind coupling function—a combination of solar wind/IMF parameters providing the best fit with geomagnetic activity. The most important factors responsible for geomagnetic activity are the solar wind velocity (V_{sw}) and IMF B_z component, measured in the solar-magnetospheric coordinate system. Additional parameters responsible for geomagnetic activity are the IMF azimuthal component (IMF B_y) and solar wind density (or pressure).

Most known coupling functions are the product of the solar wind speed and IMF B_z:

$$F_{V_{sw}\times B_z} \sim V_{sw} \times B_z \ , \tag{10}$$

and the Akasofu coupling function:[2,13]

$$F_{\text{Akasofu}} \sim V_{sw}\, B_{yz}^2 \sin^4(\theta/2) \ , \tag{11}$$

where B_{yz} is the IMF in the y-z plane and θ is the clock angle between the z (northward) axis and the $\mathbf{B}_{yz}$ vector. The Akasofu function was introduced to measure the energy flux from the solar wind to the magnetosphere. Therefore, for the correlation of upstream solar wind/IMF data with ground magnetic or electric fields, some modifications of the Akasofu function are commonly used; e.g., the Kan-Lee coupling function:[18]

$$F_{\text{Kan-Lee}} \sim V_{sw}\, B_{yz} \sin^2(\theta/2) \ . \tag{12}$$

These coupling functions show relatively good correlation for some time intervals but fail for others. Recently, Lyatsky et al. proposed a theoretically-deduced coupling function linking upstream solar wind data to geomagnetic activity.[5] They used the Perreault-Akasofu method[13] and took into account a scaling factor due to polar cap expansion while increasing a reconnected magnetic flux in the dayside magnetosphere. The coupling function obtained shows good correlation with geomagnetic activity indices but is dependent on the solar cycle. For moderate and high solar activity, the coupling function may be written in the following form:

$$F_\alpha = a V_{sw} B_{yz}^{1/2} \sin^2(\theta/2) \ , \tag{13}$$

where a is a coefficient. If V_{sw} is measured in km/s and B_{yz} in nT, the coefficient $a = 0.01$. The F_α coupling function is different from coupling functions used earlier, mainly by the power of B_{yz}, which is a result of the conservation of reconnected magnetic flux. This coupling function shows an effective ionospheric electric field in the region of open (reconnected) field lines computed with accounting for the scaling factor.

To test equation (13), Lyatsky et al. wrote a coupling function in the general form[5]

$$F_\alpha \sim V_{sw}^m \, B_{yz}^n \sin^\alpha(\theta/2) \ , \tag{14}$$

where m, n, and α are arbitrary values. This coupling function is related to electric and magnetic fields in the region of open magnetic field lines; therefore, the PC index was chosen for the analysis which shows the magnetic field in the polar cap. Then, the correlation coefficients were computed for this index versus this coupling function for different values of m, n, and α. They found that for moderate and high solar activity, the best correlation between the F_α coupling function and the PC index occurs near $m \approx 1$ and $n \approx 0.5$ for all values of α, which is well consistent with the theoretical equation (13), and the maximum R^2 is near $\alpha \approx 2$. That is consistent with the coupling function, equation (13). However, the formula for the best-fit coupling function was found to be dependent on the solar activity level. For solar minimum, the best correlation with geomagnetic activity takes place for $F_\alpha{}^\gamma$, where $\gamma \approx 1.4$.

The F_α coupling function may be improved while accounting for the effect of solar wind pressure/viscosity on geomagnetic activity. This effect was discussed earlier by many researchers.[19] The following coupling function was used:

$$F = F_\alpha + F_{visc} \ , \tag{15}$$

where the term $F_{visc} = b\, n^{1/4} V_{sw}{}^{3/2}$ is accounting for a contribution from viscous interaction of the solar wind with the geomagnetic field that becomes especially significant for small or northward IMF. Tsurutani and Gonzalez[19] reported that the viscosity contributed up to 10% of the summary convection while Borovsky and Funsten[20] found this contribution to be up to 20%. The formula for F_{visc} has been derived from dimensional arguments, which leads to $F_{visc} \sim n^{1/4} V_{sw}{}^{3/2}$. If the solar wind velociety (V_{sw}), the IMF, and the solar wind number density (n) are measured in km/s, nT, and cm^{-3}, respectively, the coefficients $a = 0.01$ and $b = 2 \times 10^{-4}$. The coupling function (F) means an 'effective' electric field in the polar ionosphere, measured in mV/m.

The coupling function in equation (15) shows better correlation with geomagnetic activity indices than the coupling function in equation (13). However, it does not yet eliminate the dependence on the solar cycle. The coupling function (F) in equation (15) is appropriate for moderate and high solar activity; however, for solar minimum, the better correlation with geomagnetic activity indices takes place for $F^{1.4}$.

The solar cycle effect may be significantly reduced while using the dimensionless coupling function:

$$F^* = c \ F^2/(F + C)^2 \ , \tag{16}$$

where F is derived from equation (15), the factor c is chosen equal to 100 (for convenience), and the factor $C = 26$ was derived from experimental data to provide the best-fit correlation of the F^* function with the PM and PC geomagnetic activity indices. The coupling function (F^*) provides very good correlation with geomagnetic activity for any levels of solar and geomagnetic activity as demonstrated in the next section. In this study, this dimensionless coupling function (F^*) was used.

Note that the correct choice of the coupling function is very important for improving the correlation of upstream solar wind parameters with geomagnetic activity indices and related events in the Earth's magnetosphere and ionosphere.

3.2 Correlation Between Polar Magnetic and Polar Cap Indices and Various Coupling Functions

As mentioned above, the main difference between the PM index and the existing PC index is that the PM index is accounting for the contribution from the transpolar current to geomagnetic activity even when the transpolar current is significantly deviated from its average direction. This leads to a strong increase in the correlation between the PM index and both upstream solar wind/IMF data and key ground-measured parameters such as CPC potential and Joule heating in the high-latitude ionosphere, as will be shown.

For this analysis, the hourly mean data of the PM and PC indices and upstream solar wind/IMF data, shifted to the magnetospheric bow shock position, were used. For computing the coupling function, the OMNI dataset was used, which includes the measurements of upstream solar wind/IMF data measured with the Wind or the Advanced Composition Explorer satellites, located predominantly near the $L1$ libration point toward the Sun. The PM/PC indices were compared with the coupling function(s) and averaged for the same and next hour; i.e., the correlation PM(t) or PC(t) with the coupling function (F) was investigated where $F = 0.5\ [F(t) + F(t - 1\ \text{hr})]$, which provides the best correlation.

The correlation between the PM/PC indices and the $V_{sw} B_z$ coupling function is commonly worse than the correlation with other coupling functions. For instance, goodness of fit of the correlation between the PM and PC indices with $V_{sw} B_z$ is typically about 0.4 to 0.5. Correlation of the PM and PC indices with other coupling functions, mentioned above, is better.

Figures 3 and 4 show correlation patterns for (a) the PM index and (b) the PC index with the Kan-Lee[18] coupling function, and (c) the PM index and (d) the PC index with the Lyatsky et al.[5] coupling function for 2001 and 2002 yr, respectively. Goodness of fit (R^2) of the correlation of the PM and PC indices with the Kan and Lee coupling function is about 0.59 and 0.51 for 2001, and 0.59 and 0.54 for 2002, respectively. Goodness of fit of the correlation between the PM and PC indices with the Lyatsky et al. coupling function is about 0.67 and 0.61 for 2001, and 0.67 and 0.64 for 2002, respectively. Figures 3 and 4 also show that the F_α coupling function, given by equation (13), provides much better correlation with both the PM and PC indices than the Kan-Lee coupling function. These figures also show that the correlation between any coupling function and PM index is better than the correlation between the same coupling function and PC index.

Figure 5 shows the correlation between the PM/PC indices and the dimensionless coupling function (F^*), derived by equation (16), for 2001 (a) and (b), and 2002 (c) and (d). This figure includes some results from figures 1 and 2. One can see that the correlation between the PM index and coupling function (F^*) shows a significant increase in goodness of fit (R^2) which reaches ~0.7, corresponding to the correlation coefficient $R \sim 0.84$. The goodness of fit for the PC index versus the F^* function is significantly less (about 0.62–0.65).

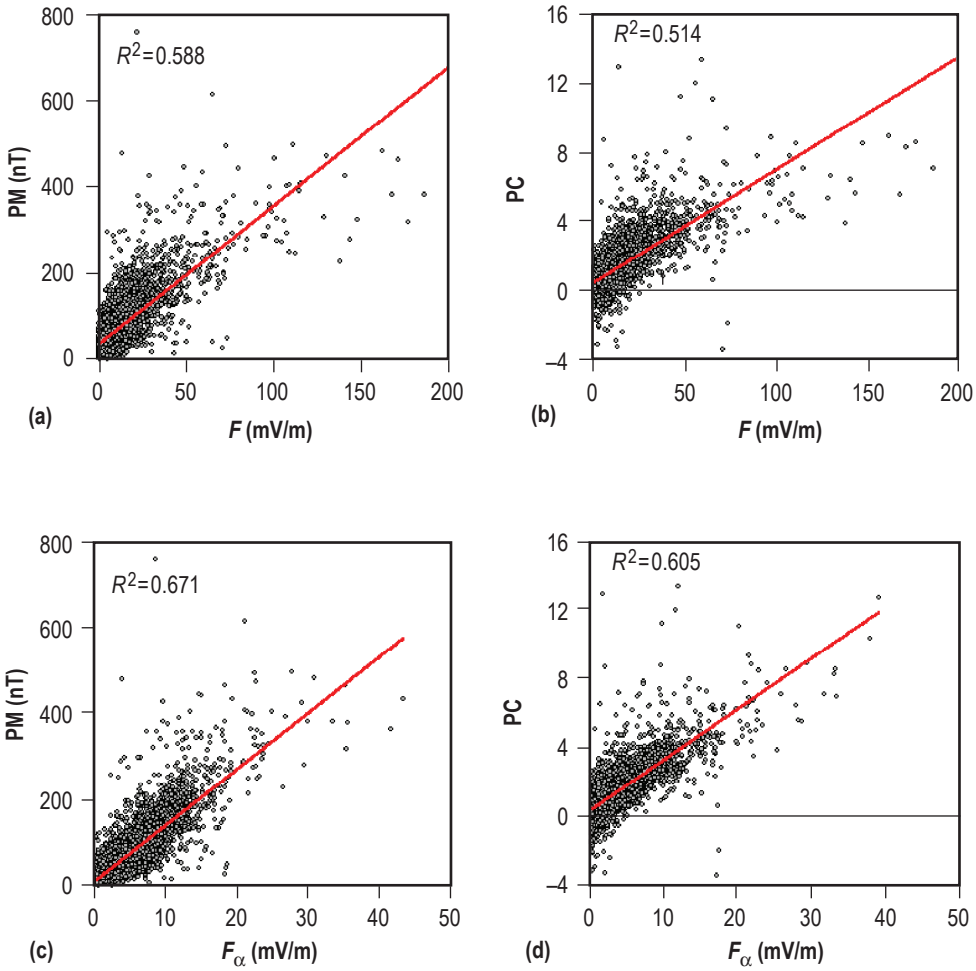

Figure 3. Correlation between PM/PC indices and upstream solar wind parameters for the Kan and Lee[18] coupling function (a) and (b), and the Lyatsky et al.[5] coupling function (c) and (d) for 2001. One can see a significant increase in goodness of fit (R^2) for the latter coupling function for both PM and PC indices.

Figures 6 and 7 show two additional examples of the correlation between the PM/PC indices and the coupling function (F^*) for low and high solar activity, respectively. Figure 6 shows the correlation between (a) the PM index and the coupling function (F^*) and (b) the PC index and the coupling function (F^*) for 1997 near solar minimum. The correlation is better than that in figure 5. In this case, the goodness of fit (R^2) reaches ~0.78 for the PM index and ~0.75 for the PC index. Figure 7 shows the correlation between (a) the PM index and the coupling function (F^*) and (b) the PC index and the coupling function (F^*) for 2000 (high solar activity). The correlation is worse than in figure 6 but yet high enough; R^2 reaches ~0.76 for the PM index and ~0.69 for the PC index.

An increase in the correlation of geomagnetic activity indices with upstream solar wind/IMF parameters for low solar activity is typical. A possible cause for this effect may be that the ranges of values of geomagnetic activity indices and the coupling functions for low solar activity are usually not large,

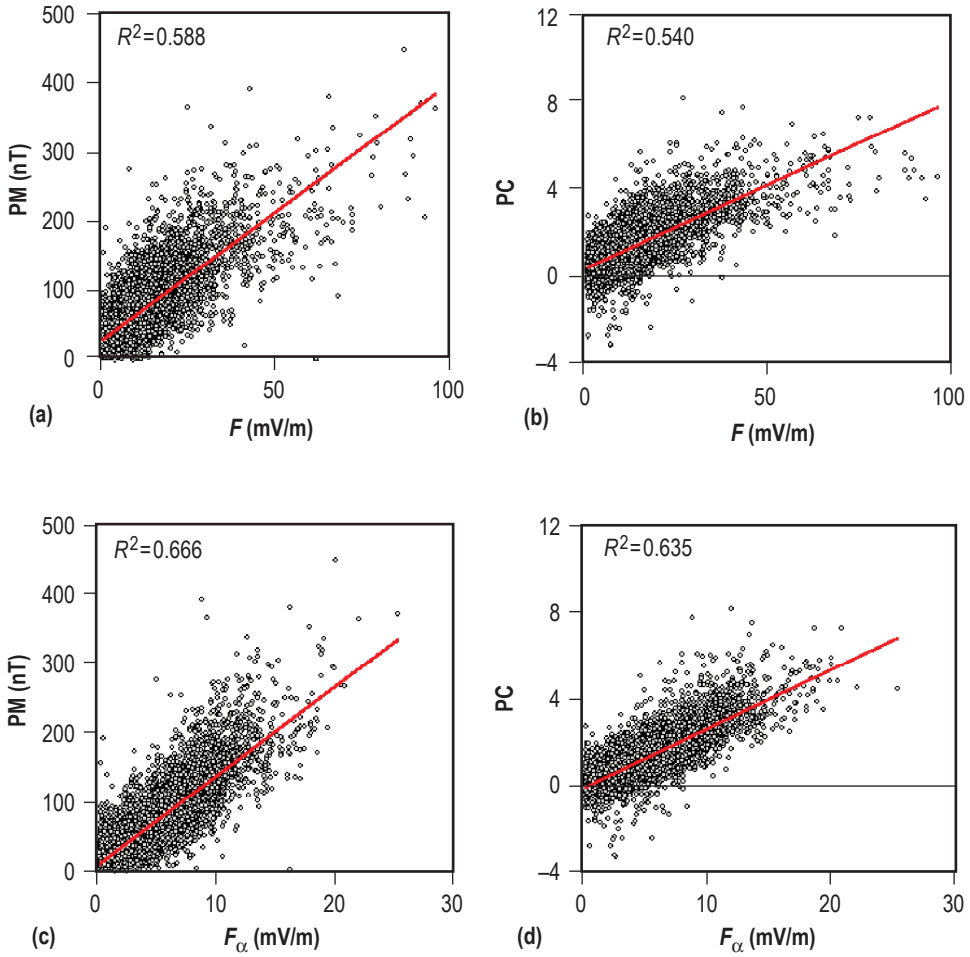

Figure 4. Correlation between PM/PC indices and solar wind parameters for the Kan and Lee[18] coupling function (a) and (b), and the Lyatsky et al.[5] coupling function (c) and (d) for 2002. Again, a significant increase is shown in the correlation between the PM/PC indices and the latter coupling function.

and the correlation between the indices and coupling function is approximately linear. During the period of high solar activity, the ranges of values of geomagnetic activity indices and the coupling function increase significantly, which may provide nonlinear effects, including the well-known 'saturation' effect in geomagnetic activity. It may reduce the correlation.

Figure 8 shows the dependence of goodness of fit (R^2) of the correlation between the PM, PC, and AL indices and the coupling function (F^*) for the 10-yr period (1995–2004). To smooth the curves, the values of R^2 in this figure were averaged for 3 yr. The PM index shows the best correlation for all years. The goodness of fit (R^2) for the PM index versus F^* varies from ~0.77 for solar minimum to ~0.7 for solar maximum. For the PC and AL indices, R^2 varies in a similar way but is significantly less in magnitude.

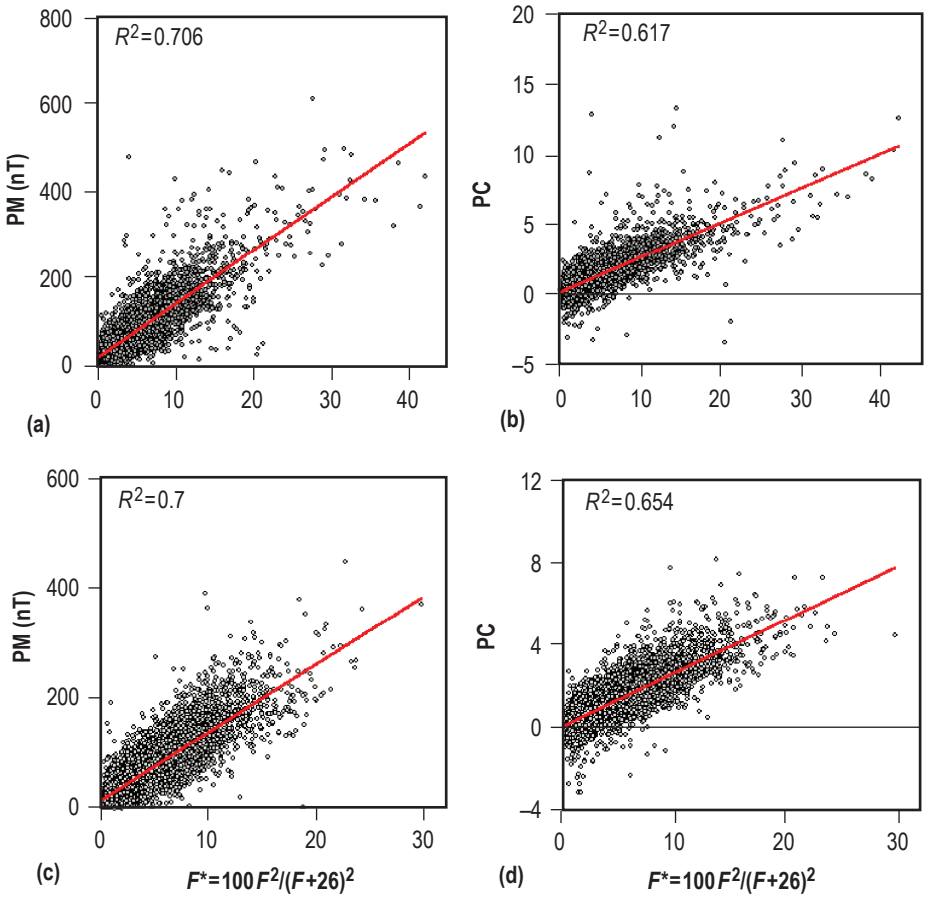

Figure 5. Correlation of the PM/PC indices with a dimensionless coupling function (F^*): (a) and (b) for 2001 and (c) and (d) for 2002. This demonstrates an increase in the correlation (against that shown in figs. 3 and 4) of both PM and PC indices with the F^* function.

Thus, one can see that the correlation between the PM index and the coupling function (F^*) in figure 8 is high enough (goodness of fit (R^2) is not less than ~0.71) and considerably higher than that for the other two indices for all years, and for low and high solar activity.

3.3 Seasonal and Universal Time Variations in Correlation Between Polar Magnetic and Polar Cap Indices and Upstream Solar Wind/Interplanetary Magnetic Field Data

The existing PC index has a strong UT/season dependence in its correlation with solar wind/IMF parameters. In contrast, the correlation of the PM index with the coupling function (F^*) shows a weak UT/season dependence. This interesting feature is demonstrated in figures 9 and 10.

Figure 9 is similar to figure 8 but is related to four summer months only (May–August). This figure also shows the dependence of goodness of fit (R^2) of the correlation of the PM, PC, and AL indices with the coupling function (F^*) for the period of 10 yr. To smooth the curves in this figure, the values of R^2 were averaged for 3 yr. One can see a strong decrease in R^2 (which drops to ~0.6) in the correlation of the

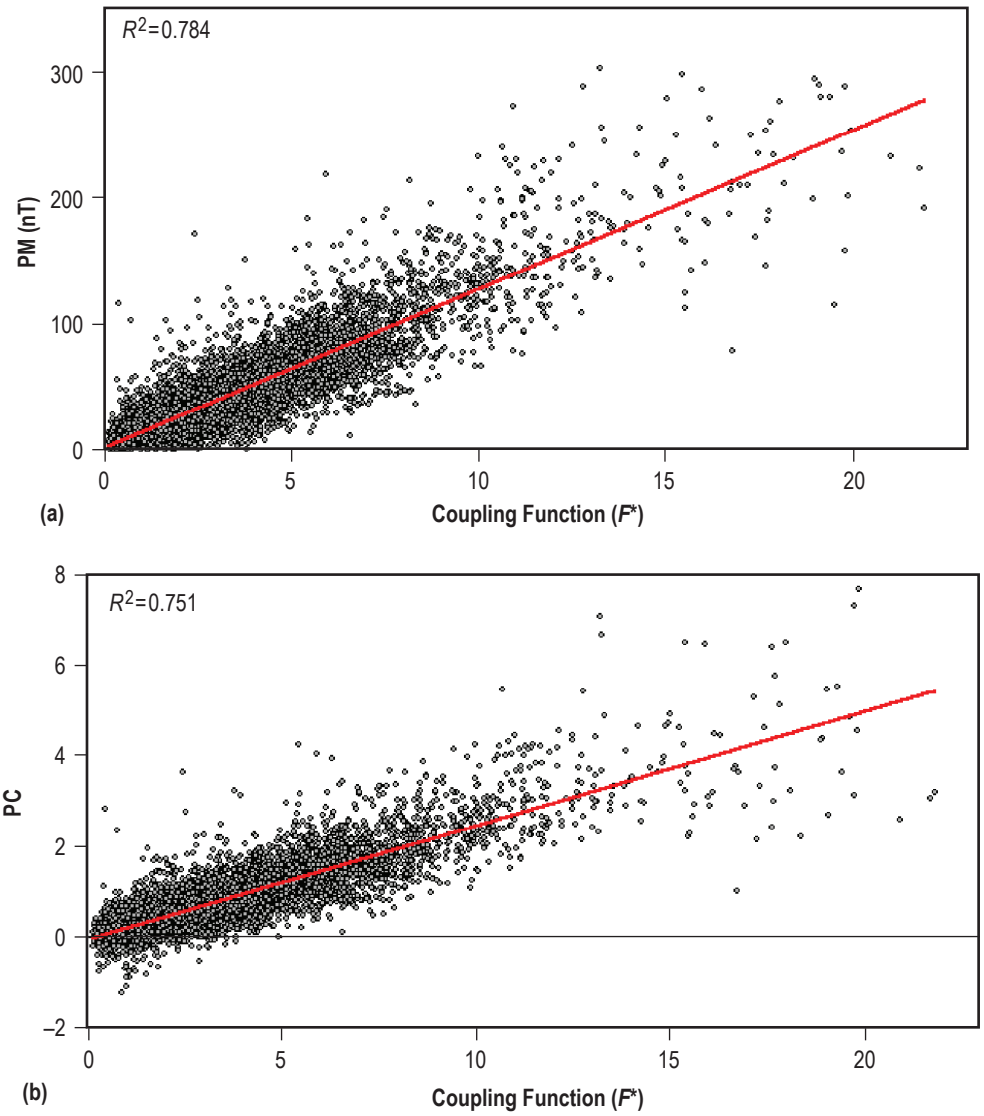

Figure 6. Correlation between (a) the PM index and coupling function (F^*) and (b) the PC index and coupling function (F^*) for 1997—related to low solar activity.

PC index with the F^* function for high solar activity, while the goodness of fit for the PM index versus the coupling function (F^*) varies insignificantly and remains at the level of $R^2 \approx 0.7$.

Figure 10 shows goodness of fit of the correlation between the PM/PC indices and the coupling function (F^*) as a function of UT for the same 10 yr (1995–2004). Panel (a) is related to low and moderate solar activity (1995–1998), while panel (b) is related to high solar activity (1999–2004). Black circles show goodness of fit (R^2) computed for PM versus F^* for each year, while red circles show R^2 for the PC index versus F^*. The correlations of the PM and PC indices with the coupling function (F^*) are close in the interval of ~4–22 UT but strongly different in the interval of 10–20 UT.

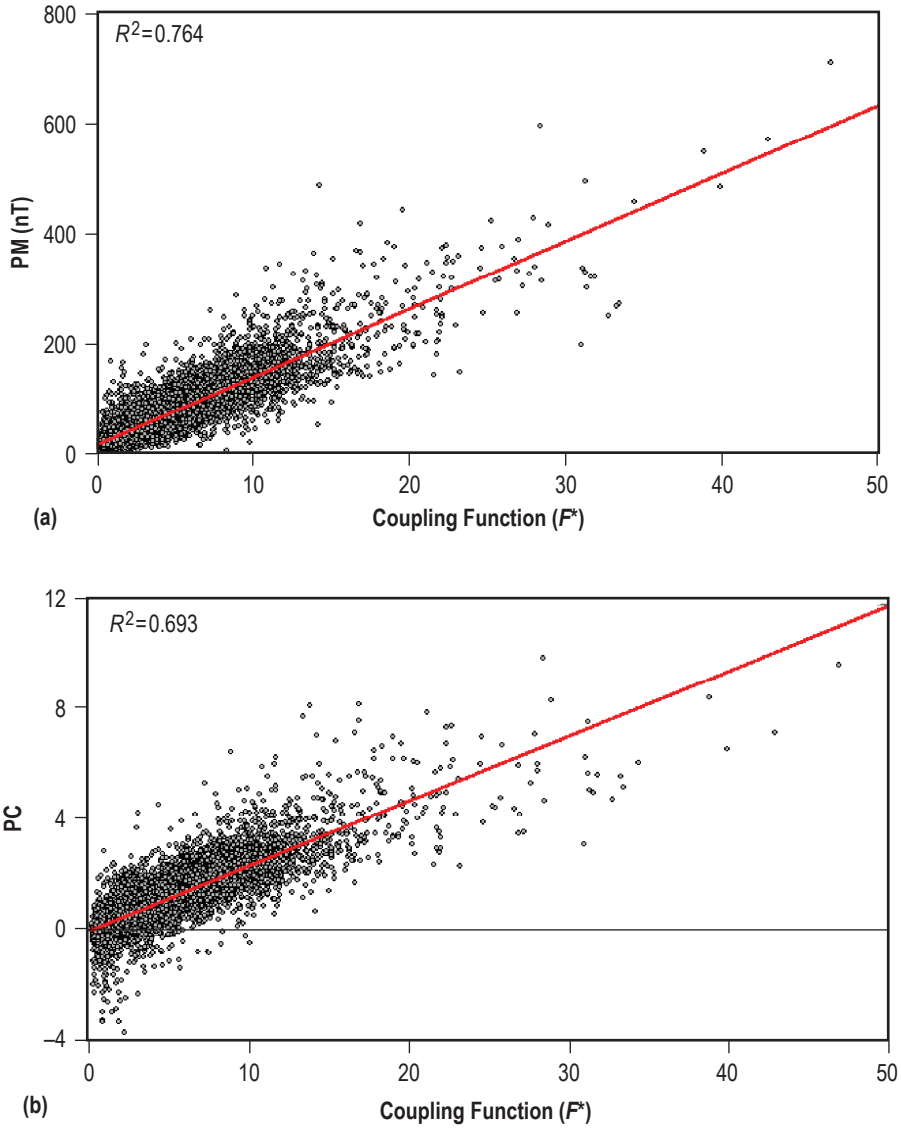

Figure 7. Correlation between (a) the PM index and coupling function (F^*) and (b) the PC index and coupling function (F^*) for 2000—related to high solar activity.

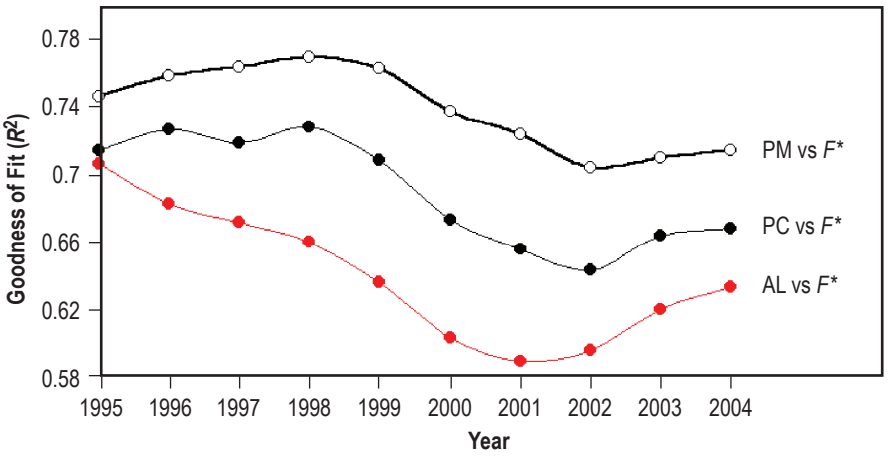

Figure 8. Solar cycle variation in correlation. Goodness of fit (R^2) of the correlation of PM, PC, and AL indices with coupling function (F^*) is shown for 10 yr (1995–2004). Correlation between PM and F^* is significantly higher than that for the PC and AL indices for all years. The average magnitude of R^2 for the correlation between the PM and F^* function is ~0.74, which corresponds to the correlation coefficient $R \approx 0.86$. Presented values of R^2 are averages for 3 yr.

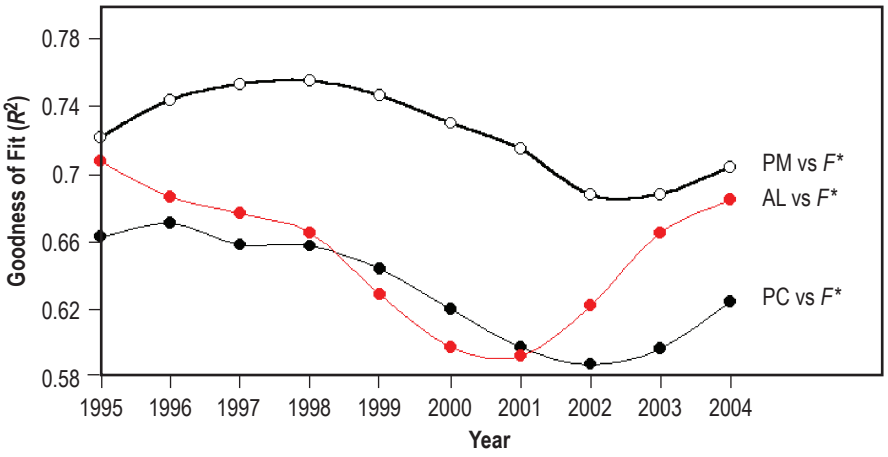

Figure 9. Summer drop in correlation. Goodness of fit (R^2) of the correlation of PM, AL, and PC indices with coupling function (F^*) is shown for summer months (May–August) for 1995–2004. This demonstrates a dramatic drop in the correlation of the PC index for the summer months while the correlation between the PM index and F^* function remains high and close to that in figure 8. Presented values of R^2 are averages for 3 yr.

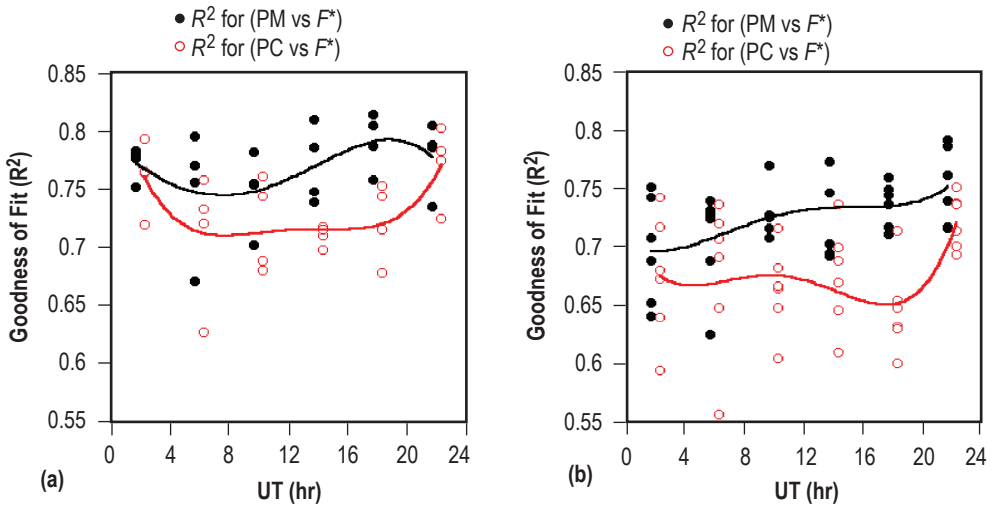

Figure 10. Universal time variation in correlation of PM/PC indices with coupling function (F^*). Shown are mean values of R^2 for 4-hr UT intervals, averaged for the following years: (a) 1995–1998 (low and moderate solar activity) and (b) 1999–2004 (high solar activity). The curves are the fourth-order polynomial fit to the data. Correlation between PC and F^* has a strong UT variation and fails in the interval of 10–20 UT while the correlation between the PM and F^* function remains high or even increases in this UT sector.

4. CORRELATION WITH AURORAL ELECTROJET AL INDEX AND SUBAURORAL Kp INDEX

4.1 Correlation With Auroral Electrojet AL Index

The AL index is based on measuring negative (southward in the Northern Hemisphere) variations in the geomagnetic field horizontal component at 12 geomagnetic observatories spread along an average position of the auroral zone. The AL index shows substorm activity in the auroral zone, which contributes significantly through the substorm-related, field-aligned currents to the magnetic field in the polar cap.[12,21] Although the AL index shows maximal negative deviations in the magnetic field's northward component while the PM index shows rather an average geomagnetic disturbance in the polar cap, the correlation between the PM and AL indices is very good for years of low solar activity but fails for years of high solar activity.

Figures 11 and 12 show the correlation of the AL index with (a) the coupling function (F^*) and (b) the PM index for 1995 (low solar activity) and 1998 (moderate solar activity), respectively. One can see the high correlation between the AL and PM indices ($R^2 \approx 0.8$ in fig. 11 and ≈ 0.73 in fig. 12), which is even better than the correlation between the AL index and the coupling function (F^*).

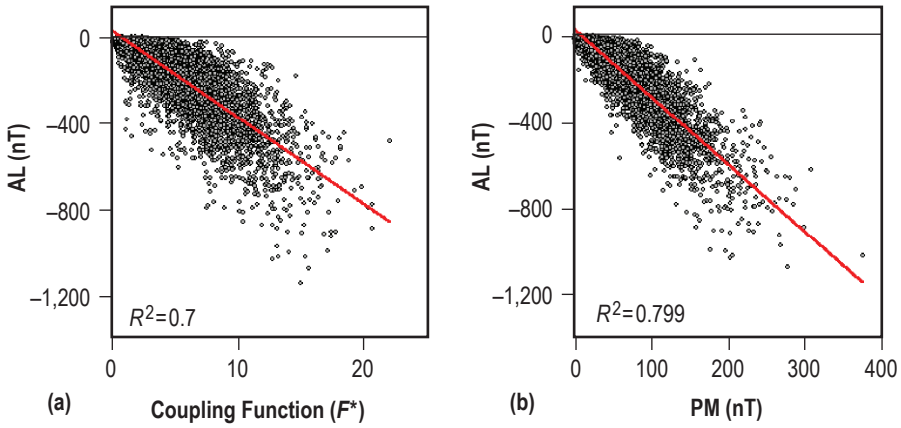

Figure 11. Correlation of (a) the AL index with coupling function (F^*) and (b) the AL index with the PM index for 1995. Correlation between the AL and PM indices is significantly higher ($R^2 \approx 0.8$ that corresponds to $R \approx 0.89$) than that between the AL and coupling function (F^*).

The correlation between the AL and PM indices decreases during solar maximum, probably due to the expansion of the auroral zone out off the position of geophysical observatories responsible for providing the AL index.[9,10] For high solar activity, the PM index—calculated using data from both overhead and remote field-aligned currents—may provide more reliable information on auroral electrojet than the AL index does for these periods.

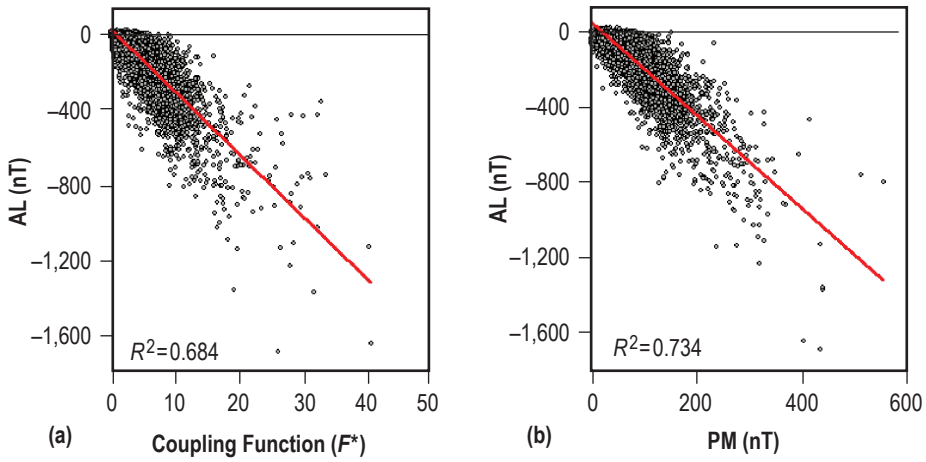

Figure 12. Correlation of (a) the AL index with coupling function (F^*) and (b) the AL index with the PM index for 1998—related to moderate solar activity. The correlation between the AL and PM indices remains high ($R^2 \approx 0.73$ that corresponds to $R \approx 0.86$).

4.2 Correlation With Subauroral Kp Index

The three-hourly Kp index shows geomagnetic activity at subauroral and middle latitudes. This index is widely used as an important input parameter for modeling magnetospheric and ionospheric processes. The Kp index, however, shows low correlation with other existing geomagnetic activity indices. It is interesting that the Kp index shows good correlation with the PM index. Note that the Kp index is a nonlinear (log) function of geomagnetic activity, and while comparing it with other indices, the best correlation takes place not just for the Kp index but for $Kp^{1.5}$.

An example of the correlation between (a) $Kp^{1.5}$ and the PM index and (b) $Kp^{1.5}$ and the PC index is shown in figure 13, related to the year 2000 (high solar activity). One can see that the correlation between the 3-hr mean values of $Kp^{1.5}$ and the related 3-hr mean PM/PC indices is much better for the PM index. Goodness of fit (R^2) between $Kp^{1.5}$ and PM is ~0.67; that is much higher than that for $Kp^{1.5}$ versus the PC (~0.57).

Figure 14 shows goodness of fit (R^2) of the correlation of $Kp^{1.5}$ with the AL, PM, and PC indices for 1995–2004. The correlation between $Kp^{1.5}$ and PM is significantly better than for the other two indices. To smooth the curves in this figure, the values of R^2 were averaged for 3 yr. Figure 14 demonstrates once more that the PM index is more appropriate for measurement and prediction of global geomagnetic activity.

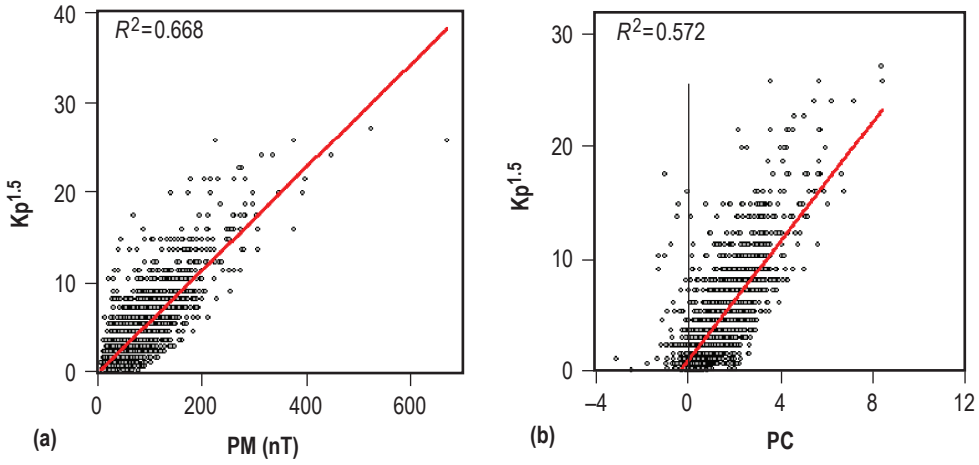

Figure 13. Correlation of (a) the Kp index with the PM index and (b) the Kp index with the PC index. Correlation between 3-hr values of $Kp^{1.5}$ and PM/PC indices for the year 2000—related to high solar activity. Goodness of fit (R^2) between $Kp^{1.5}$ and PM is much better than that for $Kp^{1.5}$ versus PC.

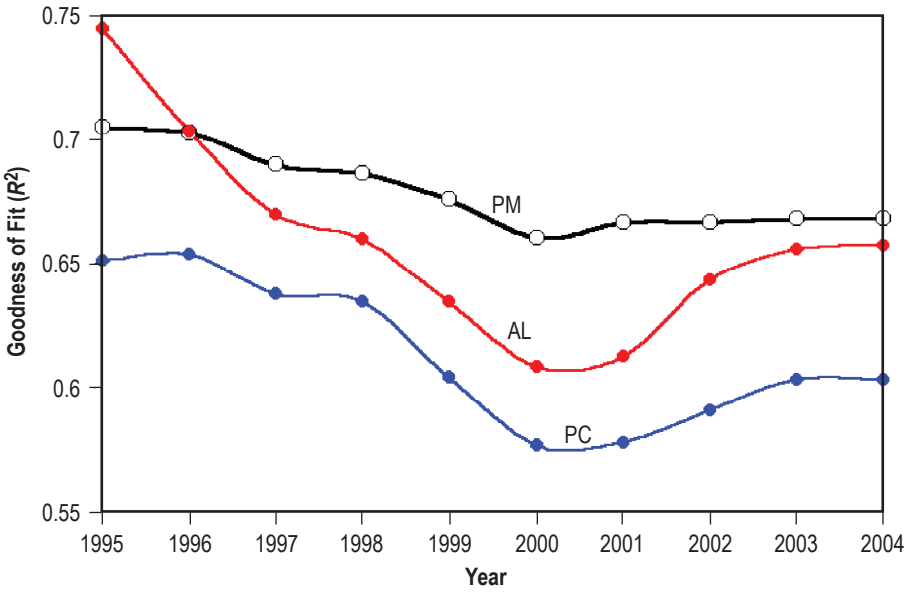

Figure 14. Goodness of fit (R^2) of the correlation of $Kp^{1.5}$ with AL, PM, and PC indices for 1995–2004. The correlation between $Kp^{1.5}$ and PM is significantly better than that for the other two indices. Presented values of R^2 are averages for 3 yr.

5. CORRELATION WITH CROSS-POLAR-CAP POTENTIAL DROP AND JOULE HEATING

5.1 Introduction

The CPC electric potential and Joule heating of high-latitude ionosphere are two key parameters that are widely used for modeling the magnetosphere, ionosphere, and thermosphere.[7,8,22–24] The CPC voltage shows electric energy flux entering the dayside ionosphere from the solar wind. The total hemispheric Joule heating shows the energy flux released in the ionosphere and heating the neutral atmosphere. Joule heating in the ionosphere produces the expansion of the atmosphere that significantly affects thermospheric dynamics and satellite orbits. According to Knipp et al.,[25] the solar extreme ultraviolet radiation on average provides ~78%, the Joule heating ~16%, and energetic particle precipitation about 5%–8% of the total power coming to the Earth's ionosphere, while during strong geomagnetic disturbances, the contribution from Joule heating becomes a predominant source of atmospheric heating. Therefore, the prediction of both CPC voltage and global Joule heating is highly important.

Permanent measurements of the CPC voltage and total Joule heating are not yet possible. The SuperDARN Doppler measurements of the $\mathbf{E}\times\mathbf{B}$ ionospheric plasma drift cannot provide permanent monitoring of ionospheric convection due to the strong dependence of radio wave reflection on ionospheric conditions. Any radar provides a reliable convection flux through the polar cap in some percent of operation time only. Other methods, including measurements with spacecraft, are also unable to provide permanent monitoring for both CPC voltage and total Joule heating.

Modeling the CPC voltage and Joule heating is more successful. The assimilative mapping of ionospheric electrodynamics (AMIE) technique,[7,26,27] based on inversion of geomagnetic field measurements from a large number of geomagnetic observatories, is widely accepted as one of the best methods for deriving both CPC voltage and Joule heating. However, since this method requires assimilation of data from a large number of geomagnetic observatories, modeling results are not available in real time. Therefore, prediction of these two important parameters—CPC voltage and total Joule heating—using the upstream solar wind/IMF data and appropriate geomagnetic activity indices,[24,28,29] remains the most reliable method of near real-time monitoring these parameters. Using the PM index and the new version of the coupling function may significantly improve the prediction reliability in forecasting these parameters.

5.2 Preliminary Results

Preliminary results relating to the correlation of the PM index with CPC potential drop and Joule heating, computed with the AMIE technique, will be shown (hourly mean values of CPC potential drop and total hemispheric Joule heating for each day of 1998 provided by A. Ridley, University of Michigan).

Figure 15 shows the correlation of hourly mean values of the AMIE CPC potential drop (U) with (a) the PM index and (b) the PC index for all days of 1998. One can see that the correlation is much better for U versus the PM index ($R^2 \approx 0.78$) than that for U versus the PC index ($R^2 \approx 0.69$).

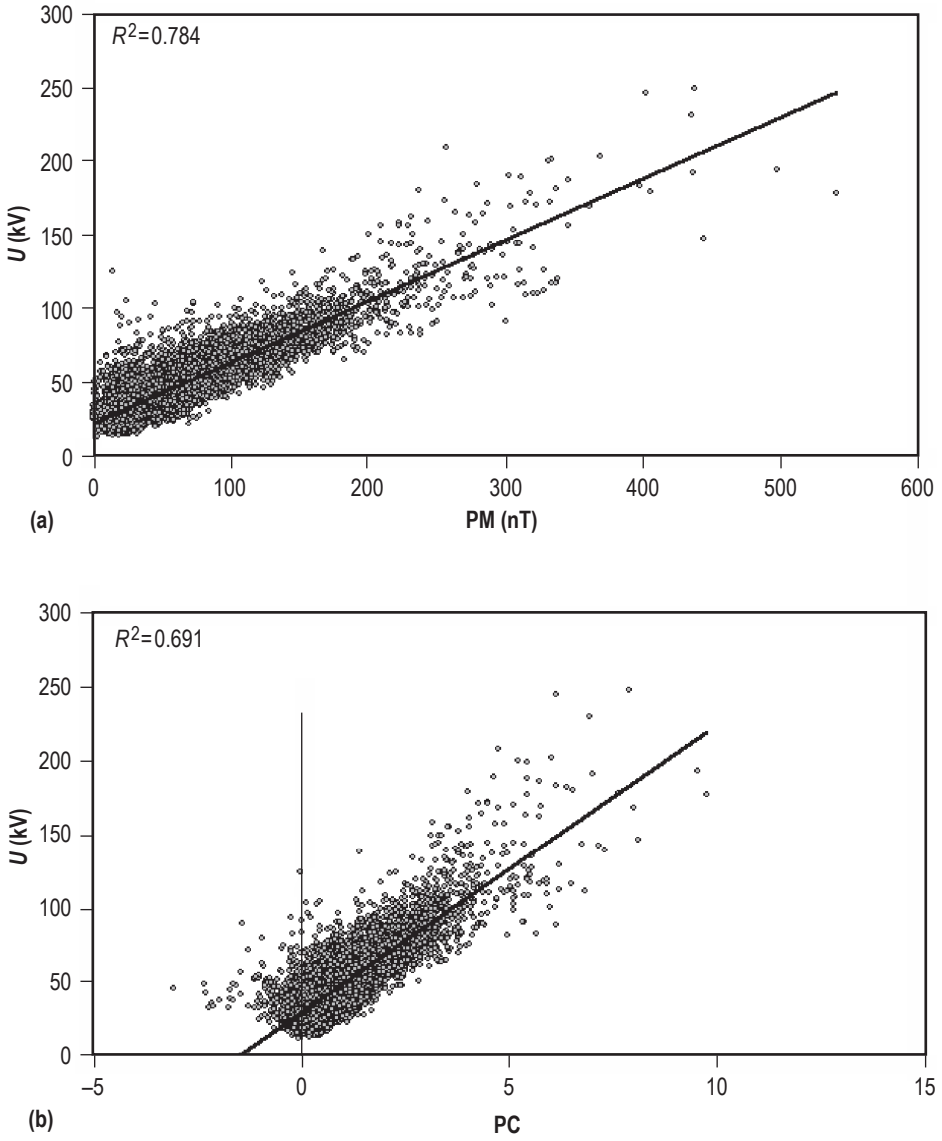

Figure 15. Correlation of hourly mean values of the AMIE CPC potential drop (U) with (a) the PM index and (b) the PC index for all days of 1998. The correlation is much better for U versus the PM index ($R^2 \approx 0.78$) than for U versus the PC index ($R^2 \approx 0.69$) (data courtesy of Aaron Ridley, University of Michigan).

Figure 16 shows the correlation of hourly mean values of the root square of the AMIE total hemispheric Joule heating with (a) the PM index and (b) the PC index for all days of 1998. The correlation is much better for $JH^{1/2}$ versus the PM index ($R^2 \approx 0.75$) than that for $JH^{1/2}$ versus the PC index ($R^2 \approx 0.68$).

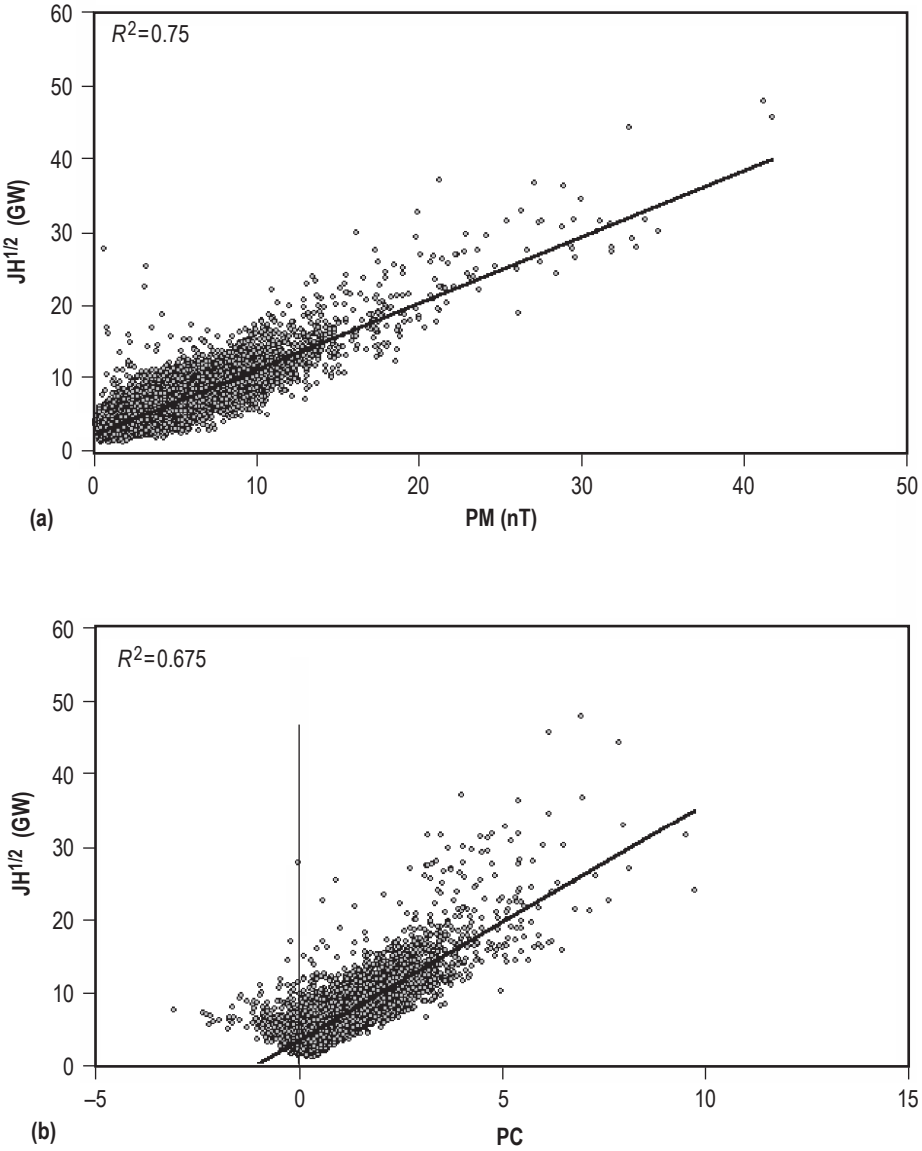

Figure 16. Correlation of hourly mean values of AMIE $JH^{1/2}$ with (a) the PM index and (b) the PC index for all days of 1998. The correlation is much better for $JH^{1/2}$ versus the PM index ($R^2 \approx 0.75$) than that for $JH^{1/2}$ versus the PC index ($R^2 \approx 0.68$) (data courtesy of Aaron Ridley, University of Michigan).

The correlation may be even more improved while accounting for both the PM index and upstream solar wind/IMF data. The comparison of predicted and actual values of the CPC voltage and Joule heating is presented in figure 17. This figure shows the correlation between the actual and predicted hourly mean values of the CPC voltage (U) and total hemispheric Joule heating ($JH^{1/2}$) for all days of 1998. Shown here is the extremely high correlation between the predicted and actual values ($R^2 \sim 0.81$ to 0.82 that correspond to the correlation coefficient $R \approx 0.9$ and more) for both U voltage and $JH^{1/2}$. For deriving the predicted values of the CPC voltage (U) and total hemispheric Joule heating, the following simple prediction functions were used:

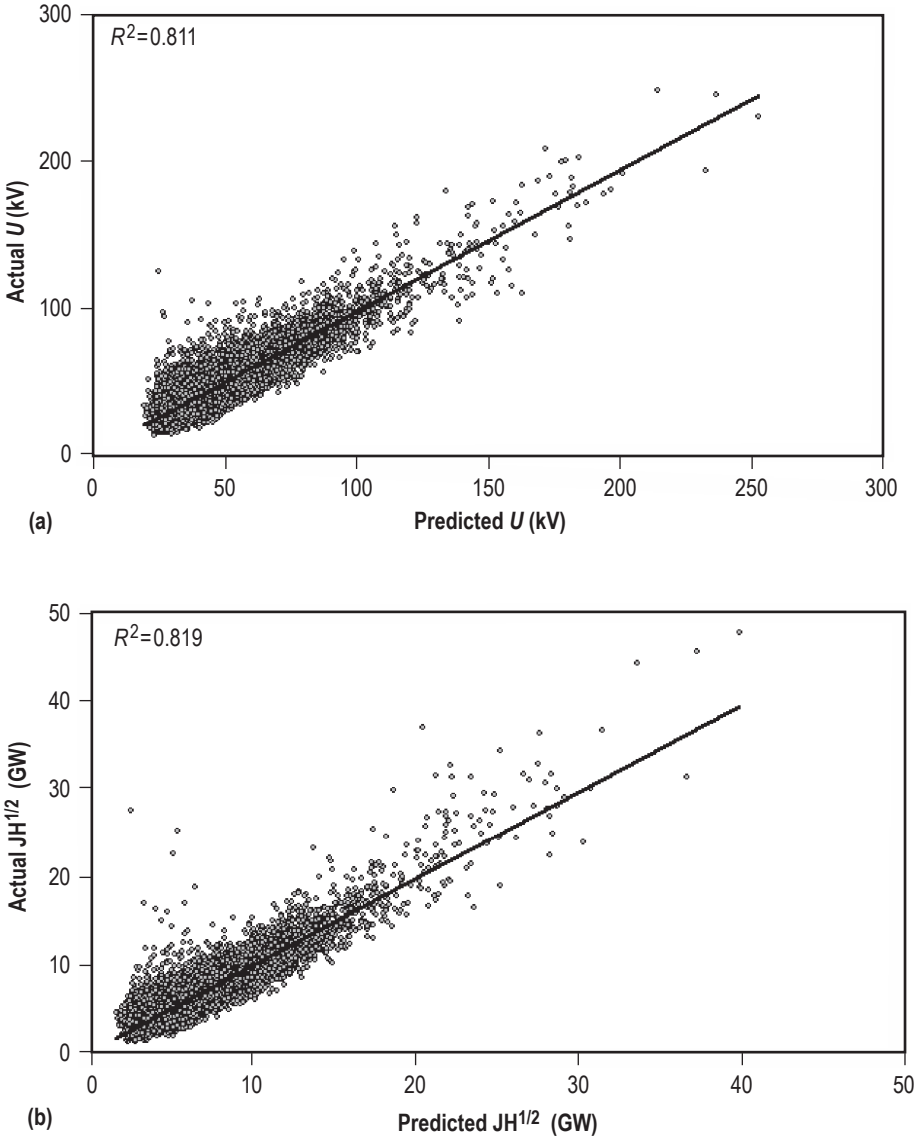

Figure 17. Correlation of the actual (AMIE) and predicted hourly mean values of the CPC voltage (U) and JH$^{1/2}$ for all days of 1998. This shows extremely high correlation ($R^2 \approx 0.81$–0.82) for both U voltage and JH$^{1/2}$ (data courtesy of Aaron Ridley, University of Michigan).

$$U_{\text{predict}}\ (\text{kV}) = 15 + 0.28\ (\text{PM} + 9\ F^*) \tag{17}$$

$$\text{JH}_{\text{predict}}\ (\text{GW}) = \left[0.9 + 0.046\ \left(\text{PM} + 9\ F^*\right)\right]^2\ , \tag{18}$$

where the PM index is measured in nT and F^* is the dimensionless coupling function derived from equation (16).

6. CONCLUSIONS

Prediction of geomagnetic activity and related events in the Earth's magnetosphere and ionosphere is an important task of the Space Weather program. Prediction reliability is dependent on a prediction method and elements included in the prediction scheme. Two main elements are a suitable geomagnetic activity index and coupling function—the combination of solar wind parameters providing the best correlation between upstream solar wind data and geomagnetic activity. The appropriate choice of these two elements is crucial for any reliable prediction model.

The PM index was computed from the magnetic field measurements from the near-pole geomagnetic observatories—Thule, Greenland, and Vostok, Antarctica, the same observatories that are used for deriving the existing PC index, but a different method for computing the PM index was used. In this study, only the PM index computed in the Northern Hemisphere was used. The most important distinction of the PM index from the existing PC index was in accounting for the contribution from the transpolar (CPC) equivalent ionospheric current to geomagnetic activity and related events even when the transpolar current deviates significantly from its average direction. This leads to a significant increase in the correlation between the PM index and both upstream solar wind/IMF data and related events in the Earth's magnetosphere and ionosphere.

The PM index shows much better correlation with the solar wind coupling function and related events than do the other indices. The correlation of the PM index with upstream solar wind/IMF data was investigated for a 10-yr period (1995–2004). The correlation coefficients for hourly mean values are very high (~0.87 to ~0.88) for low and moderate solar activity but the correlation becomes worse with increasing solar activity.

The correlation of the PM index with the AL and Kp indices, and such key ionospheric parameters as CPC voltage and Joule heating, calculated with the AMIE technique, was also investigated. These two parameters are widely used as important input parameters for modeling the magnetospheric, ionospheric, and thermospheric processes. The correlation between the PM index and the AL and Kp indices is high for low solar activity. The correlation coefficient (R) for the PM index versus the AL index is ~0.9 but decreases with increasing solar activity.

The prediction function for predicting CPC voltage and Joule heating based on using both the PM index and upstream solar wind/IMF data allows a significant increase in the reliability of the prediction of these important parameters. The correlation coefficients between the actual and predicted values of these parameters are ~0.9 and higher.

Thus, the new polar magnetic index of geomagnetic activity and the new version of the coupling function provide a significant increase in the reliability of predicting geomagnetic activity and such key parameters as CPC voltage and total Joule heating in a high-latitude ionosphere, which play an important role in the development of geomagnetic and other activities in the Earth's magnetosphere and are widely used as key input parameters in modeling magnetospheric, ionospheric, and thermospheric processes.

REFERENCES

1. Klimas, A.J.; Vassiliadis, D.; Baker, D.N.; and Valdivia, J.A.: "Data-Derived Analogues of the Solar Wind-Magnetosphere Interaction," *Phys. Chem. Earth,* Vol. 24, No. 1, pp. 37–44(8), 1999.

2. Akasofu, S.-I.: "Energy Coupling Between the Solar Wind and the Magnetosphere," *Space Sci. Rev.,* Vol. 28, pp. 121–190, 1981.

3. Vassiliadis, D.; Klimas, A.J.; Baker, D.N.; and Roberts, D.A.: "A Description of the Solar Wind-Magnetosphere Coupling Based on Nonlinear Filters," *J. Geophys. Res.,* Vol. 100, No. A3, pp. 3495–3512, 1995.

4. Gleisner, H.; and Lundstedt, H.: "Response of the Auroral Electrojets to the Solar Wind Modeled With Neural Networks," *J. Geophys. Res.,* Vol. 102, pp. 14,269–14,278, 1997.

5. Lyatsky, W.; Lyatskaya, S.; and Tan, A.: "A Coupling Function for Solar Wind Effect on Geomagnetic Activity," *Geophys. Res. Lett.*, Vol. 34, p. L02107, doi:10.1029/2006GL027666, 2007.

6. Newell, P.T.; Sotirelis, T.; Liou, K.; et al.: "A Nearly Universal Solar Wind-Magnetosphere Coupling Function Inferred From 10 Magnetospheric State Variables," *J. Geophys. Res.*, Vol. 112, p. A01206, doi:10.1029/2006JA012015, 2007.

7. Richmond, A.D.; and Kamide, Y.: "Mapping Electrodynamic Features of the High-Latitude Ionosphere From Localized Observations: Technique," *J. Geophys. Res.,* Vol. 93, No. A6, pp. 5741–5759, 1988.

8. Papitashvili, V.O.; Belov, B.A.; Faermark, D.S.; et al.: "Electric Current Patterns in the Northern and Southern Polar Regions Parameterized by the IMF," *J. Geophys. Res.*, Vol. 99, p. 13,251, 1994.

9. Rostoker, G.: "Geomagnetic Indices," *Rev. Geophys. Space Phys.*, Vol. 10, No 4, pp. 935–950, 1972.

10. Mayaud, P.N.: "Derivation, Meaning, and Use of Geomagnetic Indices," *Geophys. Monogr.*, Vol. 22, AGU, Washington, DC, 1980.

11. Troshichev O.A.; Janzhura, A.; and Stauning, P.: "Unified PCN and PCS Indices: Method of Calculation, Physical Sense, and Dependence on the IMF Azimuthal and Northern Components," *J. Geophys. Res.*, Vol. 111, doi:10.1029/2005JA011402, 2006.

12. Lyatsky, W.; Tan, A.; and Lyatskaya, S.: "Monitoring the Auroral Electrojet From Polar Cap Stations," *J. Geophys. Res.,* Vol. 111, No. A7, p. A07202, doi:10.1029/2004JA010989, 2006.

13. Perreault, P.; and Akasofu, S.-I.: "A Study of Geomagnetic Storms," *Geophys. J. R. Astr. Soc,* Vol. 54, pp. 547–573, 1978.

14. Cliver, E.W.; Kamide, Y.; and Ling, A.G.: "Mountains Versus Valleys: Semiannual Variation of Geomagnetic Activity," *J. Geophys. Res.,* Vol. 105, No. A2, pp. 2413–2424, 2000.

15. Lyatsky, W.; Newell, P.T.; and Hamza, A.M.: "Solar Illumination as Cause of the Equinoctial Preference for Geomagnetic Activity," *Geophys. Res. Lett.*, Vol. 28, No. 12, pp. 2353–2356, 2001.

16. Mansurov, S.M.: "Characteristics of Magnetic Disturbances Produced by the IMF in the Southern Polar Cap," *Geomag. Aeron.*, Vol. 21, p. 428, 1981.

17. Svalgaard, L.: "Polar Cap Magnetic Variations and Their Relationship With the Interplanetary Magnetic Field Structure," *J. Geophys. Res.*, Vol. 78, p. 2004, 1973.

18. Kan, J.R.; and Lee, L.C.: "Energy Coupling Function and Solar Wind-Magnetosphere Dynamo," *Geophys. Res. Lett.,* Vol. 6, p. 577, 1979.

19. Tsurutani, B.T.; and Gonzalez, W.D.: "The Efficiency of 'Viscous Interaction' Between the Solar Wind and the Magnetosphere During Intense Northward IMF Events," *Geophys. Res. Lett.*, Vol. 22, No. 6, pp. 663–666, 1995.

20. Borovsky, J.E.; and Funsten, H.O.: "Role of Solar Wind Turbulence in the Coupling of the Solar Wind to the Earth's Magnetosphere," *J. Geophys. Res.*, Vol. 108, No. A6, p. 1246, doi:10.1029/2002JA009601, 2003.

21. Huang, C.-S.: "Variations of Polar Cap Index in Response to Solar Wind Changes and Magnetospheric Substorms," *J. Geophys. Res.,* Vol. 110, p. A01203, doi:10.1029/2004JA010616, 2005.

22. Khazanov, G.V.; Liemohn, M.W.; Newman, T.S.; et al.: "Self-Consistent Magnetosphere-Ionosphere Coupling: Theoretical Studies," *J. Geophys. Res.*, Vol. 108, No. A3, p. 1122, doi:10.1029/2002JA009624, 2003.

23. Weimer, D.R.: "Improved Ionospheric Electrodynamic Models and Application to Calculating Joule Heating Rates," *J. Geophys. Res.*, Vol. 110, p. A05306, doi:10.1029/2004JA010884, 2005.

24. McHarg, M.; Chun, F.; Knipp, D.; et al.: "High-Latitude Joule Heating Response to IMF Inputs," *J. Geophys. Res.*, Vol. 110, p. A08309, doi:10.1029/2004JA010949, 2005.

25. Knipp, D.; Tobiska, W.; and Emery, B.: "Direct and Indirect Thermospheric Heating Sources for Solar Cycles 21–23," *Solar Physics*, Vol. 224, No. 1-2, pp. 495–505, October 2005.

26. Lu, G.; Richmond, A.D.; Emery, B.A.; and Roble, R.G.: "Magnetosphere-Ionosphere-Thermosphere Coupling: Effect of Neutral Winds on Energy Transfer and Field-Aligned Current," *J. Geophys. Res.,* Vol. 100, No. A10, pp. 19,643–19660, 1995.

27. Ridley, A.J.; and Kihn, E.A.: "Polar Cap Index Comparisons With AMIE Cross-Polar Cap Potential, Electric Field, and Polar Cap Area," *Geophys. Res. Lett.*, Vol. 31, p. L07801, doi:10.1029/2003GL019113, 2004.

28. Chun, F.K.; Knipp, D.J.; McHarg, M.G.; et al.: "Polar Cap Index as a Proxy for Hemispheric Joule Heating," *Geophys. Res. Lett.,* Vol. 26, No. 8, pp. 1101–1104, 1999.

29. Chun, F.K.; Knipp, D.J.; McHarg, M.G.; et al.: "Joule Heating Patterns as a Function of Polar Cap Index," *J. Geophys. Res.*, Vol. 107, No. A7, p. 1119, doi:10.1029/2001JA000246, 2002.

REPORT DOCUMENTATION PAGE

Form Approved
OMB No. 0704-0188

1. AGENCY USE ONLY *(Leave Blank)*	2. REPORT DATE	3. REPORT TYPE AND DATES COVERED
	October 2007	Technical Publication

4. TITLE AND SUBTITLE

Prediction of Geomagnetic Activity and Key Parameters in High-Latitude Ionosphere—Basic Elements

5. FUNDING NUMBERS

6. AUTHORS

W. Lyatsky* and G.V. Khazanov

7. PERFORMING ORGANIZATION NAME(S) AND ADDRESS(ES)

George C. Marshall Space Flight Center
Marshall Space Flight Center, AL 35812

8. PERFORMING ORGANIZATION REPORT NUMBER

M–1205

9. SPONSORING/MONITORING AGENCY NAME(S) AND ADDRESS(ES)

National Aeronautics and Space Administration
Washington, DC 20546–0001

10. SPONSORING/MONITORING AGENCY REPORT NUMBER

NASA/TP—2007–215079

11. SUPPLEMENTARY NOTES

Prepared by the Science and Exploration Research Office, Science and Mission Systems Office
*Oak Ridge Associated Universities, Oak Ridge, TN

12a. DISTRIBUTION/AVAILABILITY STATEMENT

Unclassified-Unlimited
Subject Category 46
Availability: NASA CASI 301–621–0390

12b. DISTRIBUTION CODE

13. ABSTRACT *(Maximum 200 words)*

Prediction of geomagnetic activity and related events in the Earth's magnetosphere and ionosphere is an important task of the Space Weather program. Prediction reliability is dependent on the prediction method and elements included in the prediction scheme. Two main elements are a suitable geomagnetic activity index and coupling function—the combination of solar wind parameters providing the best correlation between upstream solar wind data and geomagnetic activity. The appropriate choice of these two elements is imperative for any reliable prediction model. The purpose of this work was to elaborate on these two elements—the appropriate geomagnetic activity index and the coupling function—and investigate the opportunity to improve the reliability of the prediction of geomagnetic activity and other events in the Earth's magnetosphere. The new polar magnetic index of geomagnetic activity and the new version of the coupling function lead to a significant increase in the reliability of predicting the geomagnetic activity and some key parameters, such as cross-polar cap voltage and total Joule heating in high-latitude ionosphere, which play a very important role in the development of geomagnetic and other activity in the Earth's magnetosphere, and are widely used as key input parameters in modeling magnetospheric, ionospheric, and thermospheric processes.

14. SUBJECT TERMS

space weather prediction, geomagnetic activity index, solar wind, interplanetary magnetic field, cross-polar cap potential drop

15. NUMBER OF PAGES

40

16. PRICE CODE

17. SECURITY CLASSIFICATION OF REPORT	18. SECURITY CLASSIFICATION OF THIS PAGE	19. SECURITY CLASSIFICATION OF ABSTRACT	20. LIMITATION OF ABSTRACT
Unclassified	Unclassified	Unclassified	Unlimited

National Aeronautics and
Space Administration
IS20
George C. Marshall Space Flight Center
Marshall Space Flight Center, Alabama
35812